Targeted Exon Sequencing in Usher Syndrome Type I

Kinga M. Bujakowska,[1] Mark Consugar,[1] Emily Place,[1] Shyana Harper,[2] Jaclyn Lena,[1] Daniel G. Taub,[1] Joseph White,[1] Daniel Navarro-Gomez,[1] Carol Weigel DiFranco,[2] Michael H. Farkas,[1] Xiaowu Gai,[1] Eliot L. Berson,[1,2] and Eric A. Pierce[1,2]

[1]Ocular Genomics Institute, Massachusetts Eye and Ear Infirmary, Harvard Medical School, Boston, Massachusetts, United States
[2]Berman-Gund Laboratory for the Study of Retinal Degenerations, Harvard Medical School, Massachusetts Eye and Ear Infirmary, Boston, Massachusetts, United States

Correspondence: Eric A. Pierce, Massachusetts Eye and Ear, 243 Charles Street, Boston, MA 02114, USA; eric_pierce@meei.harvard.edu.

Submitted: July 5, 2014
Accepted: November 16, 2014

Citation: Bujakowska KM, Consugar M, Place E, et al. Targeted exon sequencing in Usher syndrome type I. *Invest Ophthalmol Vis Sci.* 2014;55:8488–8496. DOI:10.1167/iovs.14-15169

Purpose. Patients with Usher syndrome type I (USH1) have retinitis pigmentosa, profound congenital hearing loss, and vestibular ataxia. This syndrome is currently thought to be associated with at least six genes, which are encoded by over 180 exons. Here, we present the use of state-of-the-art techniques in the molecular diagnosis of a cohort of 47 USH1 probands.

Methods. The cohort was studied with selective exon capture and next-generation sequencing of currently known inherited retinal degeneration genes, comparative genomic hybridization, and Sanger sequencing of new USH1 exons identified by human retinal transcriptome analysis.

Results. With this approach, we were able to genetically solve 14 of the 47 probands by confirming the biallelic inheritance of mutations. We detected two likely pathogenic variants in an additional 19 patients, for whom family members were not available for cosegregation analysis to confirm biallelic inheritance. Ten patients, in addition to primary disease–causing mutations, carried rare likely pathogenic USH1 alleles or variants in other genes associated with deaf-blindness, which may influence disease phenotype. Twenty-one of the identified mutations were novel among the 33 definite or likely solved patients. Here, we also present a clinical description of the studied cohort at their initial visits.

Conclusions. We found a remarkable genetic heterogeneity in the studied USH1 cohort with multiplicity of mutations, of which many were novel. No obvious influence of genotype on phenotype was found, possibly due to small sample sizes of the genotypes under study.

Keywords: Usher syndrome, retinitis pigmentosa, hearing loss, retina, genetics, next-generation sequencing, selective exon capture, molecular diagnostic

Usher syndrome type 1 (USH1, MIM#276900) is characterized by the combination of retinitis pigmentosa (RP), profound congenital deafness, and vestibular ataxia. The syndrome is transmitted by the autosomal recessive mode and currently there are six genes associated with this syndrome: *Myosin VIIA* (*MYO7A,* MIM#276903),[1] *Usher syndrome 1C* (*USH1C, Harmonin,* MIM#605242),[2] *Cadherin-23* (*CDH23,* MIM#605516),[3] *Protocadherin −15* (*PCDH15,* MIM#605514),[4] *Usher syndrome 1G* (*Sans, USH1G,* MIM#607696),[5] and *Calcium and integrin binding family member 2* (*CIB2,* MIM#605564).[6] It is estimated that USH1 affects approximately 5% of all RP patients[7] and has a prevalence of up to 2 out of 100,000 people in the United States and Europe.[8–11]

The proteins encoded by USH1 genes locate to distinct structures in the photoreceptors and in the inner-ear cochlea. In primate photoreceptors, five USH1 proteins (MYO7A, CDH23, PCDH15, Harmonin, and Sans) were recently shown to localize to the calyceal processes, which are actin-based structures in the periciliary region of the photoreceptors.[12] The function of these calyceal structures is unclear; they might have a structural role supporting the photoreceptor outer segments or be involved in the fine-tuning of photoreceptor signaling. Calyceal processes are not present in all vertebrates and their absence in rodents may account for the subtle retinal phenotypes in most of the USH1 murine models, in which hearing and vestibular phenotypes are profound but retinal function appears normal.[13–19] To date only one knock-in mouse model carrying the *USH1C* c.216G>A Acadian founder mutation has shown a clear early onset dual impairment of vision and hearing.[20] In mouse retinae, the USH1 proteins locate to the transition zone and the periciliary regions of the photoreceptor inner segments, where they are thought to participate in protein transport.[13,15] In the ear, USH1 proteins are involved in the maturation of the stereocilia in the auditory hair cells of the inner-ear cochlea, where they form tip links between the stereocilia.[6,12]

The purpose of this study was to characterize genetically a cohort of 47 Usher 1 patients using targeted exon sequencing of all currently known inherited retinal degeneration (IRD) genes, along with comparative genomic hybridization (CGH) array and next-generation sequencing (NGS) data analysis to detect deletions,[21] as well as Sanger sequencing of novel exons found in the USH1 genes detected through the recently reported human retinal transcriptome.[22] Here, we also present phenotypes of these probands at their initial visits.

Materials and Methods

USH1 Patient Cohort

A total of 47 USH1 probands and eight available affected siblings were clinically examined in the Electroretinography Service at the Massachusetts Eye and Ear Infirmary. Patients underwent a full ophthalmic examination that included best corrected Snellen visual acuity, visual field testing on the Goldmann perimeter with the V-4e white test light, dark adaptation testing performed after 45 minutes of dark adaptation with an 11° white test light in the Goldmann-Weekers dark adaptometer, and full-field electroretinographic (ERG) testing with assessment of 0.5-Hz ERG amplitude and 30-Hz ERG amplitude, as previously described.[23] After patients signed informed consent, blood samples were collected from patients and available family members for DNA extraction. To our knowledge, all probands were unrelated. The study protocol adhered to the tenets of the Declaration of Helsinki and was approved by the Institutional Review Boards of Massachusetts Eye and Ear Infirmary and Harvard Medical School.

Targeted Exon Sequencing

Paired-end/multiplexable targeted enrichment capture libraries (Illumina, Inc., San Diego, CA, USA) were generated according to standard methods (BRAVO SureSelect Automated Library Prep and Capture System; Agilent Technologies, Santa Clara, CA, USA). Targeted enrichment included all currently known monogenic inherited retinal degeneration genes (RetNet; https://sph.uth.edu/retnet/ [in the public domain]; Consugar et al., unpublished observations, 2014). Targeted enrichment sample analysis was performed on an NGS platform (MiSeq; Illumina, Inc.). A 12x patient sample multiplex was clustered to an average cluster density of $\sim$ 850 K clusters per mm^2 and 2 $\times$ 121 bp paired-end analyzed using Illumina's 300-cycle MiSeq Reagent Kit V2. The average depth-of-coverage per-sample was approximately $\times$100.

Next Generation Sequence Data Analysis

Sequencing data was analyzed as previously described.[24] The Burrows-Wheeler Aligner (BWA) was used to align the sequence reads to the human reference genome (GRCh37) and Samtools to remove potential duplicates and make initial single nucleotide polymorphism (SNP) and insertion-deletion identifications.[25,26] Custom and publicly available variant filtering programs were applied to remove likely false-positive calls.[27,28] The resulting variant calls were annotated using a custom human base-pair codon resource and public resources (UCSC Genome Browser, http://genome.ucsc.edu/ [in the public domain]; ENSEMBL, http://www.ensembl.org/index.html [in the public domain]; 1000 Genomes Project, http://www.1000genomes.org [in the public domain]; Exome Variant Server [EVS], http://evs.gs.washington.edu/EVS/ [in the public domain][29]; SIFT, http://sift.jcvi.org/ [in the public domain][30]; and PolyPhen-2, http://genetics.bwh.harvard.edu/pph2/ [in the public domain][31]). Variants were filtered by frequency (<0.15%) based on EVS and dbSNP database. The frequency cutoff was chosen based on the most common arRP mutation present in USH2A c.2276G>T; p.(Cys759Phe) present (EVS frequency 20/12986 alleles). Nonsynonymous, nonsense mutations, potential splice site changes, and rare synonymous variants were considered. Rare synonymous changes were evaluated in terms of the possibility of affecting splicing. Low coverage regions (less than $\times$10) from genetically unsolved individuals were Sanger sequenced.

Variant Classification and Validation

Sequence changes were classified as follows: pathogenic (frameshift or premature translational termination if they occur before the penultimate exon, essential splice site mutations); likely pathogenic (affecting a conserved residue and when two mutated alleles of the same gene were identified in the patient); variants of uncertain significance (if only one variant was identified in a patient and it was not a stop or frameshift mutation).

All reported variants detected with NGS were confirmed through Sanger sequencing and, where possible, cosegregation in available family members was performed. Regions of interest were PCR amplified (HotFire polymerase; SolisBioDyne, Tartu, Estonia); purified (ExoSap-IT; Affymetrix, Santa Clara, CA, USA); and sequenced (BigDye Terminator v3.1, ABI 3730xl; Life Technologies, Grand Island, NY, USA). Patients were considered as solved only if they carried two likely pathogenic mutations in *trans* as proven by cosegregation analysis or by separate NGS reads.

Variant annotations were done according to the following transcripts: NM_022124.5 (*CDH23*), NM_000260.3 (*MYO7A*), NM_033056.3 (*PCDH15*), NM_153676.3 (*USH1C*) and NM_173477.2 (*USH1G*), where cDNA position is indicated considering A from the ATG start codon as the first nucleotide. The nomenclature was verified with an online tool (Mutalyzer; https://mutalyzer.nl/ [in the public domain]). All new variants will be deposited in the Leiden Open Variation Database (http://www.lovd.nl/3.0/home [in the public domain]).

Deletion Detection From Next Generation Sequencing

Coverage metrics of all the USH1 exons against control samples analyzed in the same NGS runs were compared using the publicly available Exome Hidden Markov Model (XHMM) software package.[21] Data were processed by the procedure outlined by the authors (depth of coverage analysis, filtering for high GC content, principal component analysis [PCA], normalizing and mean centering with PCA output, normalization and centering by z score). The output from XHMM gave a list of possible copy number variations (CNVs).

CGH Array

Comparative genomic hybridization array enriched with high-density probes against the RetNet disease genes was designed with an online tool (eArray, 4 $\times$ 180 K microarray; Agilent Technologies). The probes in the known Usher genes were on average 308 bp apart. This high density enables single exon deletions if more than one probe targets the exon. Samples were prepared using sex-matched control gDNA provided with the kit according to standard methods (SureTag Complete DNA Labeling Kit; Agilent Technologies). Analysis with CGH was done using commercial software (CytoGenomics; Agilent Technologies).

Novel Usher I Gene Exons

Eleven new exons in the USH1 genes were detected and eight of them were Sanger sequenced. Genomic coordinates of the novel exons or novel exon/intron boundaries of the USH1 genes were taken from human retina transcriptome data[22], which were made available at: http://oculargenomics.meei.harvard.edu/index.php/ret-trans/110-human- retinal-transcriptome.

In Silico Splicing Prediction

To evaluate the effect of mutations on splicing, the following online splicing prediction tools were used: Human Splicing

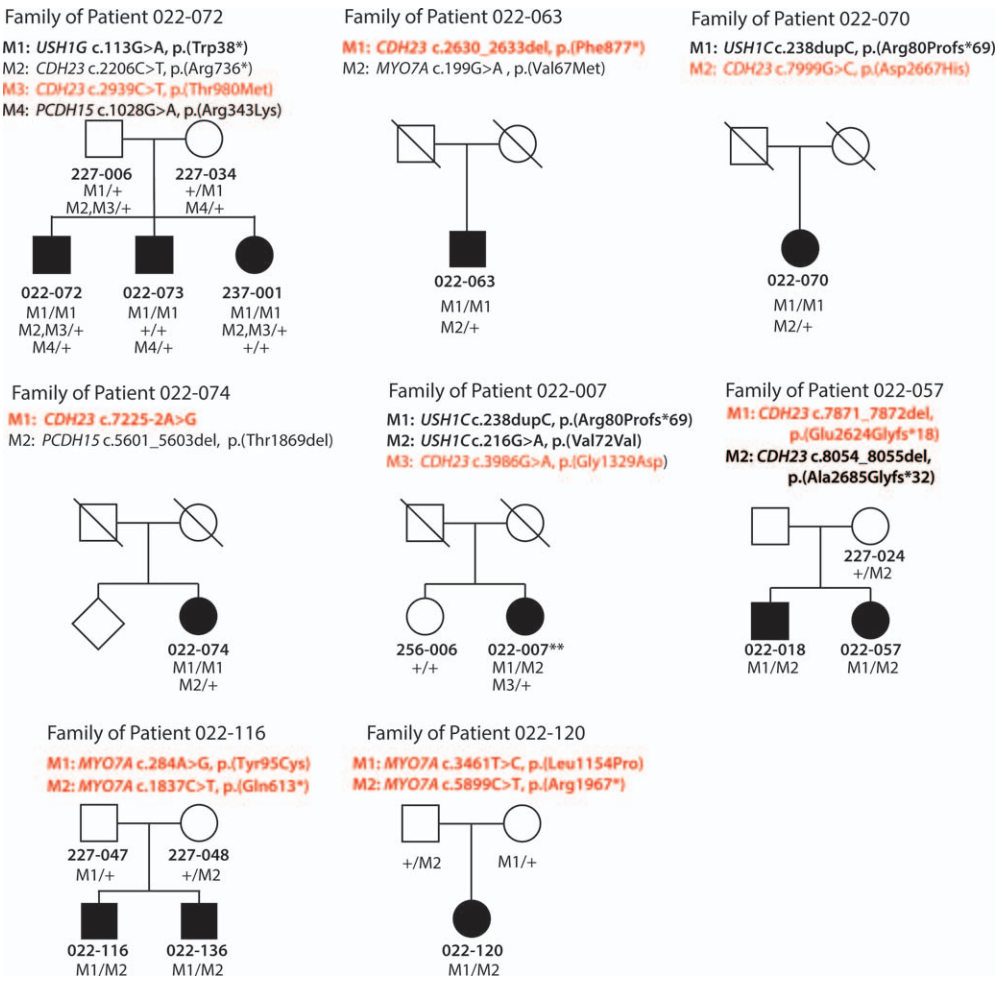

Figure 1. Pedigrees of patients carrying multiple rare variants in USH1 genes and cosegregation analysis of new mutations. *Red*: New rare mutations. *Bold*: Primary disease-causing mutations. *Circles*: Females. *Squares*: males. *Filled symbols*: Affected family members. ** Due to the unavailability of parents' DNA and taking advantage of the close proximity of the primary mutations, the biallelic inheritance was confirmed by analyzing the NGS data, where consistently the two mutations appeared on different reads.

Finder (http://www.umd.be/HSF/ [in the public domain][31]) and NNSplice (http://www.fruitfly.org/seq_tools/splice.html [in the public domain]).[32]

Results

The studied USH1 cohort of 47 probands includes 40 never-before reported patients and an additional seven unsolved cases from a previous study of mutation screening in *MYO7A*.[33] Through targeted IRD gene sequencing and Sanger sequencing-based cosegregation analysis, we found the molecular genetic basis for disease in 14 patients (Fig. 1, see Supplementary Table S1 for genotypes of all patients with two USH1 mutations). Nineteen additional patients carried two mutations considered as likely pathogenic, for whom additional family members were not available (Supplementary Table S1). Fourteen patients carried either one mutated allele in an USH1 gene or no USH1 gene variants at all.

In total, we identified 42 pathogenic mutations in USH1 genes, of which 17 were novel; these included frameshift, nonsense, and essential splice site mutations (Fig. 2, Table 1). Four new variants were considered as likely pathogenic changes and these included two missense changes and two extended splice site changes. Two novel missense changes were identified in *MYO7A*, the c.284A>G leading to a p.(Tyr95Cys) substitution in a conserved motor domain and the c.3461T>C leading to a p.(Leu1154Pro) substitution in the conserved myosin tail homology 4 (MyTH4) domain, which interacts with another USH1 protein, Sans[34] (Fig. 2). One extended splice site change was found in *MYO7A* (c.3631-3C>G; Table 1, Supplementary Table S1). The Human Splicing Finder tool predicted that the c.3631-3C>G is likely to alter splicing of exon 29, since it reduces the consensus value (CV) by 11.81% (CV reduction of 10% and above will likely affect the splicing) and also it abolished the SF2/ASF enhancer motif (ctg**c**/**g**agt).[31] The second splicing prediction tool NNSplice[32] did not recognize the native sequence, and therefore the influence of the mutation could not be verified with this program. This extended splice site mutation was coupled with a known nonsense mutation p.(Gln1798*)[33] and we consider that these two mutations are likely to cause Usher type I in this patient (Supplementary Table S1). Another extended splice-site variant was found in *CDH23* (c.145+6T>G). Even though the c.145+6T>G change is six nucleotides away from the donor site, this variant was predicted to abolish the splice donor site by the NNSplice algorithm. The Human Splicing Finder predicted abolition of the SRp40 splicing enhancer binding. In addition, this variant was coupled by a truncating mutation p.(Leu305Cysfs*8) and thus we considered both of the mutations as likely disease causing (Supplementary Table S1).

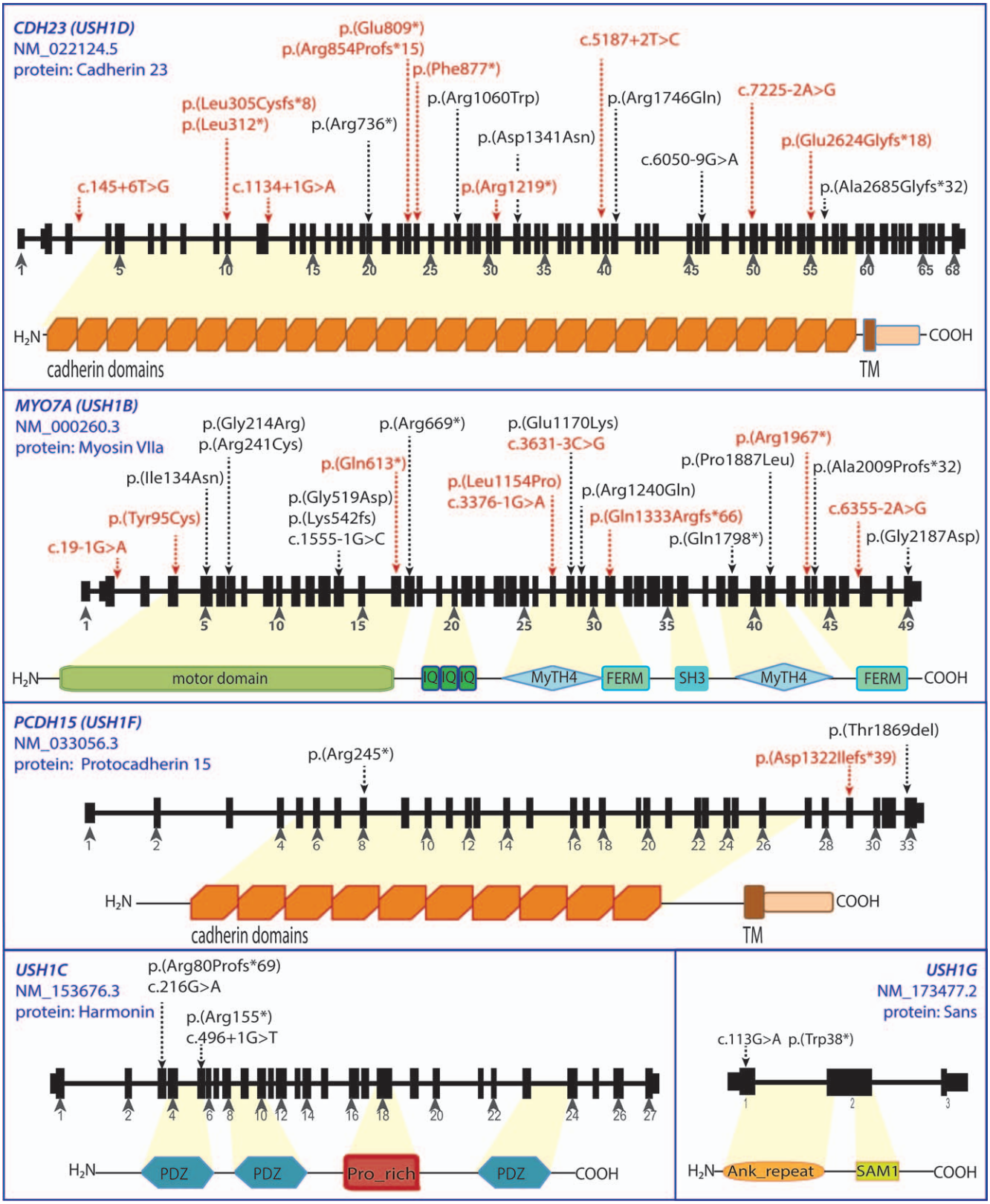

Figure 2. USH1 genes and proteins with new likely pathogenic mutations. Structures of the *MYO7A, CDH23, PCDH15, USH1C* and *USH1G* genes and proteins with the known and novel mutations identified in the studied cohort. The abbreviated protein domains represent: IQ (isoleucine glutamine calmodulin-binding motif); MyTH4 (myosin tail homology 4); FERM (4.1 protein Ezrin Radixin Moesin domain); PDZ (postsynaptic density protein [PSD95], Drosophila disc large tumor suppressor [Dlg1] and zonula occludens-1 protein [zo-1] motif); Pro_rich (proline rich domain); Ank_repeat (ankyrin repeat domain); SAM1 (sterile alpha motif); TM (trans-membrane domain). The domains were drawn based on the Pham (http://pfam.sanger.ac.uk/ [in the public domain]) and Prosite (http://prosite.expasy.org/ [in the public domain]) online tools. *CIB2* gene/protein is not presented because no new variants were identified in this gene.

Table 1. New Likely Pathogenic Changes

GENE	Hg19 Genomic Position	Exon	cDNA Change	Protein Change	Frequency (EVS)	Pathogenicity: Reason
CDH23	chr10:g.73375337delC	10	c.913del	p.(Leu305Cysfs*8)	Absent	Pathogenic: frameshift
CDH23	chr10:g.73375362delC	10	c.934del	p.(Leu312*)	Absent	Pathogenic: nonsense mutation
CDH23	chr10:g.73377151G>A	IVS11	c.1134+1G>A	splice site	Absent	Pathogenic: essential splice site
CDH23	chr10:g.73461806G>T	23	c.2425G>T	p.(Glu809*)	Absent	Pathogenic: nonsense mutation
CDH23	chr10:g.73490301C>T	31	c.3655C>T	p.(Arg1219*)	Absent	Pathogenic: nonsense mutation
CDH23	chr10:g.73538067T>C	IVS40	c.5187+2T>C	splice site	Absent	Pathogenic: essential splice site
CDH23	chr10:g.73563176_73563177delAG	55	c.7871_7872del	p.(Glu2624Glyfs*18)	Absent	Pathogenic: frameshift
CDH23	chr10:g.73462348_73462351del	24	c.2630_2633del	p.(Phe877*)	Absent	Pathogenic: nonsense mutation
CDH23	chr10:g.73206158T>G	IVS3	c.145+6T>G	splice site	Absent	Likely pathogenic: extended splice site
CDH23	chr10:g.73559247A>G	IVS51	c.7225-2A>G	splice site	Absent	Pathogenic: essential splice site
CDH23	chr10:g.73461942delG	23	c.2561del	p.(Arg854Profs*15)	Absent	Pathogenic: frameshift
MYO7A	chr11:g.76858995A>G	4	c.284A>G	p.(Tyr95Cys)	Absent	Likely pathogenic: conserved residue change
MYO7A	chr11:g.76883833C>T	16	c.1837C>T	p.(Gln613*)	Absent	Pathogenic: nonsense mutation
MYO7A	chr11:g.76895718T>C	27	c.3461T>C	p.(Leu1154Pro)	Absent	Likely pathogenic: conserved residue change
MYO7A	chr11:g.76903169delA	31	c.3998del	p.(Gln1333Argfs*66)	Absent	Pathogenic: frameshift
MYO7A	chr11:g.76919517C>T	43	c.5899C>T	p.(Arg1967*)	1/12370	Pathogenic: nonsense mutation
MYO7A	chr11:g.76853754G>A	IVS2	c.19-1G>A	splice site	Absent	Pathogenic: essential splice site
MYO7A	chr11:g.76895632G>A	IVS26	c.3376-1G>A	splice site	Absent	Pathogenic: essential splice site
MYO7A	chr11:g.76901062C>G	IVS28	c.3631-3C>G	splice site	Absent	Likely pathogenic: extended splice site
MYO7A	chr11:g.76923995A>G	IVS46	c.6355-2A>G	splice site	Absent	Pathogenic: essential splice site
PCDH15	chr10:g.55600099delC	29	c.3964delG	p.(Asp1322Ilefs*39)	Absent	Pathogenic: frameshift

The nomenclature is based on the following transcripts: NM_022124.5 (*CDH23*), NM_000260.3 (*MYO7A*), NM_033056.3 (*PCDH15*) and NM_153676.3 (*USH1C*), cDNA position is indicated considering A from the ATG start codon as the first nucleotide. Frequency data are given based on the Exome Variant Server (EVS). None of the positions had a lower depth of coverage than 20.

Ten new missense variants of uncertain significance (Table 2) were seen in patients who had either only one mutant USH1 allele or these were additional alleles in patients with primary disease mutations in another USH1 gene.

Nine patients carried one heterozygous likely pathogenic change in a USH1 gene and the remaining five did not carry mutations in any known USH1 gene. We have not found the missing mutant alleles by Sanger sequencing of the NGS sequence gaps or by sequencing of the eight new, non-canonical USH1 exons discovered by the human retina transcriptome study[22] (Table 3). Three novel exons (*CDH23* ex19b, ex19c and *MYO7A* ex31b) were highly repetitive and GC rich; therefore, we were not able to sequence them. We did not find any likely disease-causing deletions or duplications in these patients by using a custom design CGH array or by comparing sequence coverage of all of the USH1 exons in the unsolved patients against control samples that were sequenced in the same NGS runs using the XHMM algorithm.[21]

Of note are patients who carry primary disease causing mutations in one USH1 gene and also additional rare USH1 alleles (Fig. 1). Three affected sibs from the family of proband 022-072 carrying homozygous mutations in *USH1G* [c.113G>A (p.Trp38*)] also carried additional rare variants in other USH1 genes. The proband was most severely affected and he carried additional heterozygous variants in *CDH23* [c.2206C>T, p.(Arg736*)] and *PCDH15* [c.1028G>A p.(Arg343Lys)]. The

Table 2. New Variants With Uncertain Significance

Patient ID	Gene	Hg19 Genomic Position	Exon	cDNA Change	Protein Change	Frequency (EVS)	Notes
022-107	*CDH23*	chr10:g.73206137G>A	3	c.130G>A	p.(Glu44Lys)	Absent	Single rare variant in an USH1 gene
022-120	*CDH23*	chr10:g.73437383A>G	16	c.1685A>G	p.(Gln562Arg)	Absent	Disease due to *MYO7A* mutations
022-072	*CDH23*	chr10:g.73464873C>T	25	c.2939C>T	p.(Thr980Met)	Absent	Disease due to *USH1G* mutations
022-007	*CDH23*	chr10:g.73492014G>A	32	c.3986G>A	p.(Gly1329Asp)	4/12502	Disease due to *USH1C* mutations
022-079	*CDH23*	chr10:g.73558900G>A	51	c.7087G>A	p.(Glu2363Lys)	Absent	Disease due to *MYO7A* mutations
022-070	*CDH23*	chr10:g.73565689G>C	56	c.7999G>C	p.(Asp2667His)	1/12363	Disease due to *USH1C* mutations
022-004	*MYO7A*	chr11:g.76913417G>A	37	c.5116G>A	p.(Glu1706Lys)	Absent	Disease due to *CDH23* mutations
OGI-008-020	*MYO7A*	chr11:g.76867107G>A	3	c.440G>A	p.(Arg147His)	Absent	Single rare variant in an USH1 gene
022-038	*PCDH15*	chr10:g.55780122C>T	20	c.2581G>A	p.(Val861Met)	5/12999	Single rare variant in an USH1 gene
022-123	*USH1C*	chr11:g.17531369G>A	18	c.1547C>T	p.(Pro516Leu)	2/12968	Single rare variant in an USH1 gene

These missense changes were seen in patients who had either only one mutant allele or there were additional alleles in patients with two mutations in other USH1 genes and therefore they were classified as variants of uncertain significance. The nomenclature is based on the following transcripts: NM_022124.5 (*CDH23*), NM_000260.3 (*MYO7A*), NM_033056.3 (*PCDH15*) and NM_153676.3 (*USH1C*). cDNA position is indicated considering A from the ATG start codon as the first nucleotide. Frequency data are given based on the Exome Variant Server (EVS).

Table 3. Inferred New Exons in USH1 Genes Identified Through Retina Transcriptome Analysis[22]

Gene	Novel Exons	Exon Boundaries	Size (bp)
PCDH15	33b*	chr10:55579925-55579990	65
CDH23	19b†	chr10:73448294-73448316	22
CDH23	19c†	chr10:73448497-73448661	164
CDH23	38b	chr10:73521691-73521783	92
CDH23	48b	chr10:73554289-73554385	96
CDH23	59alt	chr10:73567424-73567457	33
MYO7A	2b	chr11:76852801-76852854	53
MYO7A	31b†	chr11:76902622-76902827	205
MYO7A		chr11:76902720-76902827	107
MYO7A	32b	chr11:76904037-76904093	56
MYO7A		chr11:76904037-76904157	120
MYO7A		chr11:76904097-76904157	60
MYO7A		chr11:76904121-76904157	36
MYO7A		chr11:76904121-76904396	275
MYO7A		chr11:76904185-76904396	211
MYO7A	44b	chr11:76919707-76919848	141
MYO7A		chr11:76919768-76919848	80
MYO7A	46b	chr11:76922819-76922976	157
MYO7A		chr11:76922819-76922982	163
MYO7A		chr11:76922819-76923094	275
MYO7A		chr11:76922819-76923150	331

*exon number is based on the transcript NM_001142771.

†Due to high GC content and highly repetitive sequence these exons were not sequenced successfully.

p.(Arg343Lys) variant in *PCDH15* is a rare variant (EVS: 5/13001 alleles) that was previously classified as unlikely to be a primary disease causing mutation (benign/likely benign in ClinVar database); however, its potential as a modifier remains to be evaluated. The less affected sibs carried mutations either in *CDH23* (sister 237-001) or *PCDH15* (brother 022-073; Fig. 1, Supplementary Table S3). One of the patients (022-063) was previously reported to carry one likely pathogenic variant in *MYO7A* [c.199G>A, p.(Val67Met)][33] and in this study we found that this patient is homozygous for the c.2630_2633del, p.(Phe877*) mutation in *CDH23* (Supplementary Table S1). Even though we cannot exclude the possibility that the p.(Val67Met) variant is likely pathogenic, the disease in this patient is due to the homozygous nonsense mutation in *CDH23*. In addition, some patients carried heterozygous variants in other genes associated with deaf-blindness (*DFNB31, GPR98, USH2A and ALMS1*); 14 such variants were identified (see Supplementary Table S2 for a list of additional variants in USH1 genes and genes associated with other forms of deaf-blindness).

Patients included in the study suffered from profound deafness since childhood and vestibular dysfunction manifested by delayed walking (after age 14 months) and/or persistent balance problems in adulthood. The majority of patients had shown retinal dysfunction when tested in early teenage years, with elevated final dark adaptation thresholds, constricted visual fields and reduced ERG amplitudes (see Supplementary Table S3 for clinical description of patients with two likely pathogenic alleles). Clinical observations on the studied cohort did not reveal substantial differences on average between patients carrying primary mutations in different USH1 genes, but our analyses were limited by small sample sizes (Table 4 and Supplementary Table S3).

Discussion

Using targeted exon sequencing of the known IRD genes in 47 Usher type I probands we were able to give a definite molecular diagnosis for 14 patients, for whom we found pathogenic mutations and we had evidence of biallelic inheritance. In addition, we found two pathogenic or likely pathogenic mutations in 19 patients, for whom we did not have family members to preform cosegregation analysis. Fourteen patients remain unsolved, of whom nine carried one heterozygous allele in a USH1 gene and five did not carry rare variants in any of the known USH1 genes. With the above results, we obtained a genetic diagnostic rate of 70% (30% definitely solved and 40% likely solved) similar to another study of Usher exome sequencing for clinical purposes,[35] implying that there are other genetic cause(s) of Usher type I to be discovered. With NGS, we identified 17 new pathogenic mutations, which included frameshift, nonsense, and essential splice site mutations, four new likely disease-causing missense and extended splice site changes and 10 additional rare variants with uncertain significance. With almost half of the identified mutations being novel, NGS had an advantage over microarray-based techniques, which detect mostly known variants.[36]

The sequencing of all the IRD genes allows for an unbiased genetic characterization of patients and for considering all the rare alleles in genes associated with the studied disease. In addition, it may help to elucidate the pattern of possible modifying alleles. We found a number of patients that apart from the primary disease-causing mutations carried additional rare USH1 alleles that may increase the severity of the disease. Furthermore some patients carried variants in other genes associated with deaf-blindness (*DFNB31, GPR98, USH2A and ALMS1*). Interaction between mutations in these genes and USH1 alleles remains to be elucidated. The influence of the increased mutation load on phenotype has previously been observed in Bardet-Biedl syndrome[37–39] and may have also an effect in Usher type I. However, larger families or larger patient cohorts combined with detailed clinical studies would have to

Table 4. Clinical Findings of Patients With Definite or Likely Pathogenic Mutations In USH1 Genes at Their Initial Visit

Gene	Mean Age of Walking, mo (*n*)	Visual Acuity OU, age (*n*)	Visual Field OU, deg² (age, *n*)	30Hz ERG OU, μV (age, *n*)	Cataract OU	Bone Spicule/ Clumped Pigmentation OU	Granular Macula OU
CDH23	22.8 (5)	20/54 (33.6, 9)	3487.9 (37.0, 7)	1.49 (36.7, 8)	4/9 patients	8/9 patients	5/9 patients
MYO7A	20.5 (10)	20/35 (23.3, 15)	6663.0 (21.8, 12)	2.90 (21.4, 13)	5/15 patients	11/15 patients	5/15 patients
USH1C	27.9 (7)	20/36 (28.9, 10)	4806.9 (28.9, 10)	1.14 (26.8, 9)	7/10 patients	8/10 patients	6/10 patients

In columns 2 through 5, *n* designates number of patients for whom clinical data was available. The values represent averages of the data from a given group of patients. Normal value for the age of walking ≤14 months; visual acuity (best corrected Snellen visual acuity), best corrected Snellen visual acuity = 20/20; Goldmann total field area to V-4e white test light ≥11,399 deg²; 30 Hz cone ERG ≥50 μV. The bone spicule or clumped pigmentation is regarded as positive if present in one or more retinal quadrants. Clinical data for each patient are summarized in Supplementary Table S1. There was only one patient with two *PCDH15* alleles, and only three patients with two *USH1G* alleles and therefore they were not included in this table.

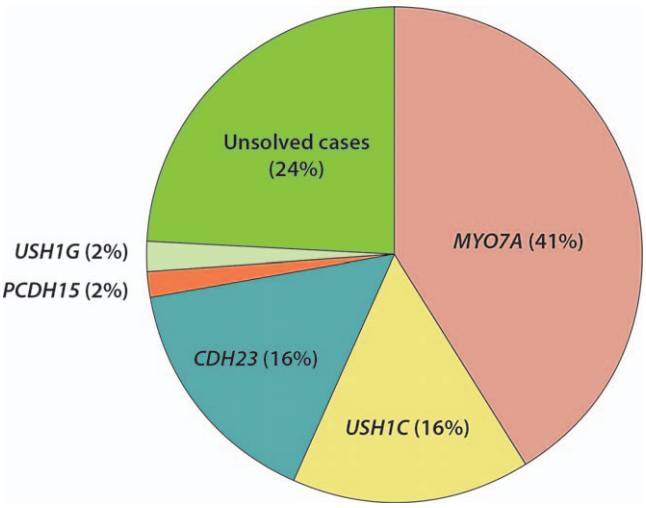

FIGURE 3. Prevalence of USH1 gene mutations in the combined cohort of 58 Usher type I patients. This cohort includes 47 studied probands and 11 previously published cases with two mutant USH1 alleles.[33] There were no patients with *CIB2* mutations in this study.

be undertaken in order to demonstrate possible epistatic effects of additional mutations in other genes associated with deaf-blindness. A thorough reporting of genetic results, including the possible modifying alleles, will in the future facilitate the analyses of the genetic factors influencing the disease severity and progression. Such epistatic effects have been suggested for other related disorders[40,41] and methods for in vivo functional analysis have been developed.[42,43]

Mutations in *MYO7A* were the most frequent in the investigated USH1 cohort (13 patients), followed by *USH1C* (nine patients) and *CDH23* (nine patients; Supplementary Table S1). By adding the previously solved 11 *MYO7A* cases,[33] we estimate that in this combined USH1 cohort, approximately 41% of patients carry mutations in *MYO7A*, that 16% carry mutations in *USH1C* and *CDH23*, and that 2% carry mutations in *USH1G* and *PCDH15* (Fig. 3). We did not identify any mutations in *CIB2*. The prevalence of *MYO7A* and *CDH23* falls within or close to the previously reported ranges in other cohorts (29% to 50% for *MYO7A* and 19% to 35% for *CDH23*).[10,44] We observed lower frequency of patients with *PCDH15* mutations, which was reported to represent 11% to 19% cases in other cohorts.[10,44] A relatively high prevalence of *USH1C* mutations was observed in this study, which in other cohorts ranges from 6% to 7%.[10] This was due to two founder mutations present in our cohort: c.216G>A (p.Val72Val), common in the French Canadian populations of Acadian origin[10,45] and the c.238dupC (p.Arg80Profs*69) mutation common in patients with European origins.[2,46]

Fourteen patients remain genetically unsolved and there are five plausible reasons for not finding the mutations in the targeted exon sequencing: (1) the sequence coverage in the targeted exon sequencing was low in some areas; (2) there are larger deletions or rearrangements not detectable by exon sequencing; (3) there are deeper intronic mutations causing aberrant splicing as shown for other genes[47,48]; (4) there are mutations in regulatory regions not targeted by our study; or (5) mutations in a gene not currently associated with Usher syndrome are responsible for the disease. The first two possibilities were explored by filling in the NGS gaps by Sanger sequencing, searching for CNVs with CGH array and NGS data analysis algorithms to detect CNVs (XHMM).[21] With these techniques, we did not detect any large deletions in the USH1 genes (deletions ranging from one exon to the whole gene). It is possible that we failed to detect some deletions with the CGH array that lie outside of the regions hybridizing the CGH probes and that the sample size was insufficient for the accurate CNV detection by the XHMM method. The methods used in this study were not adequate to detect genetic rearrangements. It has recently been demonstrated that deep intronic mutations in a gene associated with Stargardt disease, *ABCA4,* affect splicing of auxiliary regulatory exons, which were discovered through retina transcriptome analysis.[49] By Sanger sequencing of eight novel exonic features, we were not able to identify any rare variants that could be pathogenic. Sequencing of the entire genetic interval of the USH1 genes may reveal deep intronic changes, CNVs, or other genetic rearrangements, which may be disease causing as shown for other genes.[47–49] A subset of the unsolved patients may carry such changes in the USH1 genes, but there may also be new USH1 genes that have not been identified yet. Whole genome sequencing seems an adequate approach to study both possibilities as shown for the retinitis pigmentosa patients by Nishiguchi and colleagues.[50] The challenge of this approach, however, is in determining which of the large number of variants identified is pathogenic.

In summary, we found a remarkable genetic heterogeneity in the studied USH1 cohort with multiplicity of mutations, of which many were novel. More work is needed to define the course of these diseases; however, this task may prove difficult since many USH1 patients present with low visual function and complete deafness at their initial visit. With the limited sample size studied, we were not able to identify significant phenotypic differences between subjects with different genotypes, consistent with the previously reported shared retinal disease mechanism of patients with mutations in *MYO7A*, *PCDH15*, *USH2A* and *GPR98*.[51] In addition to retinal and cochlear phenotype-genotype correlations, balance and gait should also be investigated. A common indicator of the vestibular ataxia is a self-reported age of walking, which may be inaccurate. An unbiased method of sensory balance assessment will be useful to investigate the effect of different genotypes on vestibular ataxia.[52,53] Additional studies will be needed to fully understand USH1 disease and to determine therapies that can safely be pursued. A phase 1 clinical trial of lentiviral-mediated gene augmentation therapy for retinal degeneration due to *MYO7A* mutations is currently in progress to evaluate the safety of this potential treatment approach (NCT01505062).[54,55] Hopefully, the results from this study will encourage development of therapies for other USH1 genes. The success of these therapies will depend on our understanding of the disease progression and also on selecting the appropriate time-points for treatment.

Acknowledgements

The authors would like to thank the patients and their family members for their participation in this study, and Aliete Langsdorf and Maria Sousa for their experimental assistance.

Supported by grants from the National Eye Institute (EY012910), the Foundation Fighting Blindness (USA) and the Fleming Family Foundation.

Disclosure: **K.M. Bujakowska**, None; **M. Consugar**, None; **E. Place**, None; **S. Harper**, None; **J. Lena**, None; **D.G. Taub**, None; **J. White**, None; **D. Navarro-Gomez**, None; **C. Weigel DiFranco**, None; **M.H. Farkas**, None; **X. Gai**, None; **E.L. Berson**, None; **E.A. Pierce**, None

References

1. Weil D, Blanchard S, Kaplan J, et al. Defective myosin VIIA gene responsible for Usher syndrome type 1B. *Nature*. 1995; 374:60–61.

2. Verpy E, Leibovici M, Zwaenepoel I, et al. A defect in harmonin, a PDZ domain-containing protein expressed in the inner ear sensory hair cells, underlies Usher syndrome type 1C. *Nat Genet*. 2000;26:51–55.
3. Bolz H, von Brederlow B, Ramírez A, et al. Mutation of CDH23, encoding a new member of the cadherin gene family, causes Usher syndrome type 1D. *Nat Genet*. 2001;27:108–112.
4. Ahmed ZM, Riazuddin S, Bernstein SL, et al. Mutations of the protocadherin gene PCDH15 cause Usher syndrome type 1F. *Am J Hum Genet*. 2001;69:25–34.
5. Weil D, El-Amraoui A, Masmoudi S, et al. Usher syndrome type I G (USH1G) is caused by mutations in the gene encoding SANS, a protein that associates with the USH1C protein, harmonin. *Hum Mol Genet*. 2003;12:463–471.
6. Riazuddin S, Belyantseva IA, Giese APJ, et al. Alterations of the CIB2 calcium- and integrin-binding protein cause Usher syndrome type 1J and nonsyndromic deafness DFNB48. *Nat Genet*. 2012;44:1265–1271.
7. Hartong DT, Berson EL, Dryja TP. Retinitis pigmentosa. *Lancet*. 2006;368:1795–1809.
8. Rosenberg T, Haim M, Hauch AM, Parving A. The prevalence of Usher syndrome and other retinal dystrophy-hearing impairment associations. *Clin Genet*. 1997;51:314–321.
9. Hope CI, Bundey S, Proops D. Fielder a R. Usher syndrome in the city of Birmingham–prevalence and clinical classification. *Br J Ophthalmol*. 1997;81:46–53.
10. Millán JM, Aller E, Jaijo T, Blanco-Kelly F, Gimenez-Pardo A, Ayuso C. An update on the genetics of usher syndrome. *J Ophthalmol*. 2011;2011:417217.
11. Boughman JA, Vernon M, Shaver KA. Usher syndrome: definition and estimate of prevalence from two high-risk populations. *J Chronic Dis*. 1983;36:595–603.
12. Sahly I, Dufour E, Schietroma C, et al. Localization of Usher 1 proteins to the photoreceptor calyceal processes, which are absent from mice. *J Cell Biol*. 2012;199;381–399.
13. Williams D. Usher syndrome: animal models, retinal function of Usher proteins, and prospects for gene therapy. *Vision Res*. 2008;48;433–441.
14. Miyasaka Y, Suzuki S, Ohshiba Y, et al. Compound heterozygosity of the functionally null Cdh23v-ngt and hypomorphic Cdh23ahl alleles leads to early-onset progressive hearing loss in mice. *J Exp Anim Sci*. 2013;62:333–346.
15. Liu X, Udovichenko IP, Brown SD, Steel KP, Williams DS. Myosin VIIa participates in opsin transport through the photoreceptor cilium. *J Neurosci*. 1999;19:6267–6274.
16. Libby RT, Steel KP. Electroretinographic anomalies in mice with mutations in Myo7a, the gene involved in human Usher syndrome type 1B. *Invest Ophthalmol Vis Sci*. 2001;42:770–778.
17. Di Palma F, Holme RH, Bryda EC, et al. Mutations in Cdh23, encoding a new type of cadherin, cause stereocilia disorganization in waltzer, the mouse model for Usher syndrome type 1D. *Nat Genet*. 2001;27:103–107.
18. Johnson KR, Gagnon LH, Webb LS, et al. Mouse models of USH1C and DFNB18: phenotypic and molecular analyses of two new spontaneous mutations of the Ush1c gene. *Hum Mol Genet*. 2003;12:3075–3086.
19. Ahmed ZM, Kjellstrom S, Haywood-Watson RJL, et al. Double homozygous waltzer and Ames waltzer mice provide no evidence of retinal degeneration. *Mol Vis*. 2008;14;2227–2236.
20. Lentz J, Gordon W, Farris HE, et al. Deafness and retinal degeneration in a novel USH1C knock-in mouse model. *Dev Neurobiol*. 2010;70:253–267.
21. Fromer M, Moran JL, Chambert K, et al. Discovery and statistical genotyping of copy-number variation from whole-exome sequencing depth. *Am J Hum Genet*. 2012;91:597–607.
22. Farkas M, Grant G, White J, Sousa M, Consugar M, Pierce E. Transcriptome analyses of the human retina identify unprecedented transcript diversity and 3.5 Mb of novel transcribed sequence via significant alternative splicing and novel genes. *BMC Genomics*. 2013;14:486.
23. Berson EL, Rosner B, Sandberg MA, et al. A randomized trial of vitamin A and vitamin E supplementation for retinitis pigmentosa. *Arch Ophthalmol*. 1993;111:1462–1463.
24. Falk MJ, Zhang Q, Nakamaru-Ogiso E, et al. NMNAT1 mutations cause Leber congenital amaurosis. *Nat Genet*. 2012;44:1040–1045.
25. Li H, Durbin R. Fast and accurate short read alignment with Burrows-Wheeler transform. *Bioinformatics*. 2009;25:1754–1760.
26. Li H, Handsaker B, Wysoker A, et al. The sequence alignment/map format and SAMtools. *Bioinformatics*. 2009;25:2078–2079.
27. Benjamini Y, Hochberg Y. Controlling the false discovery rate: a practical and powerful approach to multiple testing. *J R Stat Soc*. 1995;57:289–300.
28. McKenna A, Hanna M, Banks E, et al. The genome analysis toolkit: a MapReduce framework for analyzing next-generation DNA sequencing data. *Genome Res*. 2010;9:1297–1303.
29. NHLBI GO Exome Sequencing Project. Exome variant server. Available at: http://evs.gs.washington.edu/EVS/. Accessed June 30, 2014.
30. Ng PC, Henikoff S. SIFT: Predicting amino acid changes that affect protein function. *Nucleic Acids Res*. 2003;31:3812–3814.
31. Desmet F-O, Hamroun D, Lalande M, Collod-Béroud G, Claustres M, Béroud C. Human Splicing Finder: an online bioinformatics tool to predict splicing signals. *Nucleic Acids Res*. 2009;37:e67.
32. Reese M, Eeckman F, Kulp D, Haussler D. Improved splice site detection in Genie. *J Comput Biol*. 1997;4:311–323.
33. Bharadwaj AK, Kasztejna JP, Huq S, Berson EL, Dryja TP. Evaluation of the myosin VIIA gene and visual function in patients with Usher syndrome type I. *Exp Eye Res*. 2000;71;173–181.
34. Cosgrove D, Zallocchi M. Usher protein functions in hair cells and photoreceptors. *Int J Biochem Cell Biol*. 2014;46;80–89.
35. Besnard T, García-García G, Baux D, et al. Experience of targeted Usher exome sequencing as a clinical test. *Mol Genet genomic Med*. 2014;2;30–43.
36. Jaijo T, Aller E, García-García G, et al. Microarray-based mutation analysis of 183 Spanish families with Usher syndrome. Invest Ophthalmol Vis Sci. 2010;51:1311–1317.
37. Katsanis N, Ansley SJ, Badano JL, et al. Triallelic inheritance in Bardet-Biedl syndrome, a Mendelian recessive disorder. *Science*. 2001:293;2256–2259.
38. Badano JL, Leitch CC, Ansley SJ, et al. Dissection of epistasis in oligogenic Bardet-Biedl syndrome. *Nature*. 2006;439:326–330.
39. Badano JL, Kim JC, Hoskins BE, et al. Heterozygous mutations in BBS1, BBS2 and BBS6 have a potential epistatic effect on Bardet-Biedl patients with two mutations at a second BBS locus. *Hum Mol Genet*. 2003;12:1651–1659.
40. Coppieters F, Casteels I, Meire F, et al. Genetic screening of LCA in Belgium: predominance of CEP290 and identification of potential modifier alleles in AHI1 of CEP290-related phenotypes. *Hum Mutat*. 2010;31:E1709–E1766.
41. Poloschek CM, Bach M, Lagreze WA, et al. ABCA4 and ROM1: implications for modification of the PRPH2-associated macular dystrophy phenotype. *Invest Ophthalmol Vis Sci*. 2010;51;4253–4265.

Investigative Ophthalmology & Visual Science

42. Samardzija M, Wenzel A, Naash M, Remé CE, Grimm C. RPE65 as a modifier gene for inherited retinal degeneration. *Eur J Neurosci*. 2006;23:1028–1034.
43. Niederriter AR, Davis EE, Golzio C, Oh EC, Tsai I-C, Katsanis N. In vivo modeling of the morbid human genome using Danio rerio. *J Vis Exp*. 2013;78:e50338.
44. Vozzi D, Aaspõllu A, Athanasakis E, et al. Molecular epidemiology of Usher syndrome in Italy. *Mol Vis*. 2011;17:1662–1668.
45. Ebermann I, Lopez I, Bitner-Glindzicz M, Brown C, Koenekoop RK, Bolz HJ. Deafblindness in French Canadians from Quebec: a predominant founder mutation in the USH1C gene provides the first genetic link with the Acadian population. *Genome Biol*. 2007;8:R47.
46. Zwaenepoel I, Verpy E, Blanchard S, et al. Identification of three novel mutations in the USH1C gene and detection of thirty-one polymorphisms used for haplotype analysis. *Hum Mutat*. 2001;17:34–41.
47. Den Hollander AI, Koenekoop RK, Yzer S, et al. Mutations in the CEP290 (NPHP6) gene are a frequent cause of Leber congenital amaurosis. *Am J Hum Genet*. 2006;79:556–561.
48. Webb TR, Parfitt DA, Gardner JC, et al. Deep intronic mutation in OFD1, identified by targeted genomic next-generation sequencing, causes a severe form of X-linked retinitis pigmentosa (RP23). *Hum Mol Genet*. 2012;21:3647–3654.
49. Braun TA, Mullins RF, Wagner AH, et al. Non-exomic and synonymous variants in ABCA4 are an important cause of Stargardt disease. *Hum Mol Genet*. 2013;22:5136–5145.
50. Nishiguchi KM, Tearle RG, Liu YP, et al. Whole genome sequencing in patients with retinitis pigmentosa reveals pathogenic DNA structural changes and NEK2 as a new disease gene. *Proc Natl Acad Sci U S A*. 2013;110:16139–16144.
51. Jacobson SG, Cideciyan AV, Aleman TS, et al. Usher syndromes due to MYO7A, PCDH15, USH2A or GPR98 mutations share retinal disease mechanism. *Hum Mol Genet*. 2008;17;2405–1415.
52. Khattar V, Hathiram B. The clinical test for the sensory interaction of balance. *Int J Otorhinolaryngol Clin*. 2012;4:41–45.
53. Horak FB, Wrisley DM, Frank J. The Balance Evaluation Systems Test (BESTest) to differentiate balance deficits. *Phys Ther*. 2009;89:484–498.
54. Lopes VS, Boye SE, Louie CM, et al. Retinal gene therapy with a large MYO7A cDNA using adeno-associated virus. *Gene Ther*. 2013;20:824–833.
55. Hashimoto T, Gibbs D, Lillo C, et al. Lentiviral gene replacement therapy of retinas in a mouse model for Usher syndrome type 1B. *Gene Ther*. 2007;14:584–594.

Investigative Ophthalmology & Visual Science